

# Tsunami Load Evaluation Based on Field Investigations of the 2011 Great East Japan Earthquake



**T. Asai & Y. Nakano**

*The University of Tokyo, Japan*

**T. Tateno**

*Kajima Corporation, Japan*

**H. Fukuyama**

*Building Research Institute, Japan*

**K. Fujima**

*National Defense Academy, Japan*

**T. Sugano**

*The Building Center of Japan, Japan*

**Y. Haga & T. Okada**

*The Japan Building Disaster Prevention Association, Japan*

## SUMMARY:

To design and construct buildings resistive to tsunami loads, quantitative evaluations of tsunami load applicable to structural design is most essential. The practical design load for tsunami shelters proposed by The Building Center of Japan in 2004 were examined through surveys of structures after the Indian Ocean Tsunami in December 2004. Nonetheless researches on tsunami load against structures based on damage observations are yet insufficient. In this paper, structures that experienced the Great East Japan Earthquake were surveyed, and the relationship between their damage, strengths, and inundation depth is quantitatively investigated to examine the design load.

*Key Words: The Great East Japan Earthquake, Tsunami, Tsunami shelter, Design load*

## 1. INTRODUCTION

To design and construct buildings resistive to tsunami loads, quantitative evaluations of tsunami load applicable to structural design is most essential. The design guidelines for tsunami shelters were developed by a task committee under the Japanese Cabinet Office in 2005 referring “Structural Design Method of Building to Seismic Sea Wave” (Okada et al. 2004a and 2004b), which introduced a formula to compute tsunami loads expected to act on shelters constructed on coastlines (JCO 2005). The formula was developed primarily based on laboratory tests of 2-dimensional scaled model (Asakura et al. 2000) and examined through surveys of structures after the Indian Ocean Tsunami in December 2004 (Nakano 2008). However, since researches on tsunami loads against structures based on damage observations are yet insufficient and tsunami damage caused by the 2011 Great East Japan Earthquake was devastating, quantitative evaluations of tsunami loads are currently in urgent need in terms of tsunami disaster prevention in the future. The authors therefore made extensive damage surveys of structures that experienced the tsunami caused by the 2011 Great East Japan Earthquake to investigate the relationship between their lateral strength and observed damage, and to verify the appropriateness of the design formula. In this paper, the outline of the damage surveys and investigated results on design tsunami loads are presented.

## 2. OUTLINE OF DAMAGE SURVEYS

### 2.1. Surveyed Areas

Damage surveys were made in Tohoku area (from Hachinohe city in Aomori Prefecture to Soma city in Fukushima Prefecture as shown in Fig. 1) from the beginning of April through the end of June, 2011.

### 2.2. Survey Strategy

Surveys were made to review the overall damage in the areas, and to record structural dimension and



**Figure 1.** Surveyed areas

reinforcement arrangement etc. to further investigate the relationship between their lateral strength and tsunami load that acted on them since they met the following three conditions:

- (1) The lateral strength of the surveyed structures could be simply estimated based on the structural properties obtained on site, because (i)their sectional properties (cross-sectional size, reinforcement arrangement, etc.) were measured; (ii)their damage (or collapse) mechanism was simple and the boundary between damaged and intact part of the structure was not complicated; and (iii)they were small and/or regular enough in their plan and height that their lateral strength could be calculated through simple modeling and assumptions.
- (2) The tsunami inundation depth was clearly found on the surveyed site through water marks left on building's walls, where it was defined and measured as the water depth above the ground level at the building's site.
- (3) The tsunami load could be simply estimated because the surveyed structures were located in areas close to the coastlines and the direct effects by tsunami attack were the primary source of the damage.

In this paper, the measured tsunami inundation depth  $\eta_m$  corresponding to the design tsunami inundation depth  $h$  (m), which will be described later, was defined not to be affected by the local water splash-up on the front face of buildings. This is because the design tsunami inundation depth is generally simulated neglecting local effects of buildings. The measured tsunami inundation depth  $\eta_m$  is, therefore, defined as:

- (1) the tsunami trace found on a rear or side walls of a building in flatland areas from Ishinomaki city to Soma city because it was higher on a front face than on the other faces due to water splash-up, and
- (2) the highest tsunami trace around a building in saw-tooth Sanriku area from Kuji city to Onagawa town because no major differences in tsunami height were found among traces on all sides of exterior walls. This is due primarily to the fact that the flow velocity was not high enough at its maximum inundation depth in Sanriku area to cause water splash-up on the front face as evidenced by the tsunami videos recorded during the event.

### 2.3. Detailed Information Recorded on Investigated Structures

Photo 1 shows the typical structures investigated in this study. Considering three conditions for detailed surveys described earlier, more than 130 structures including (a)buildings with simple configuration, (b)fence walls, (c)RC or masonry columns (bridge piers, gate piers, etc.), (d)stone monuments, (e)seawalls, and (f)steel fences, were investigated and detailed structural data were collected. They include (1)locations with GPS data, (2)topographical information of the site, (3)use and type of structure (RC, CB (concrete block), stone, etc.), (4)damage pattern, (5)tsunami inundation depth  $\eta_m$ , (6)structure and/or member dimension (B x D x H, wall thickness, etc.), (7)reinforcement arrangement (diameter, spacing, cover concrete depth, etc.), (8)general view photos, and (9)structural configurations.



**Photo 1.** Typical investigated structures (Letters (a) to (e) show categories of structures)

### 3. EVALUATION OF LATERAL STRENGTH OF INVESTIGATED STRUCTURES

#### 3.1. Lateral Strength of Buildings

The lateral strength of the buildings categorized in (a) as exemplified in Photo 1 is evaluated based on the first level screening of seismic evaluation procedure which is generally applied in Japan (JBDPA 2001), using the measured structure dimension and the material test results. Buoyant forces are neglected in the evaluation because overturned buildings are not discussed in this paper.

#### 3.2. Lateral Strength of Simple Structures

According to the damage and failure mode observed, the cracking strength  $M_c$ , the flexural yielding strength  $M_y$ , the ultimate flexural strength at rebar fracture  $M_u$ , the overturning strength  $M_{OT}$ , the sliding strength  $P_s$  are calculated for simple structures categorized in (b) through (e) described earlier.  $M_y$  and  $M_u$  of RC members are computed from Eqns. 3.1 through 3.3 that are widely applied in Japanese design practice. The mechanical properties of materials are based on their test results.

$$M_y = 0.9 a_t \sigma_y d \quad (3.1)$$

$$M_u = 0.9 a_t \sigma_u d \quad (3.2)$$

$$M_y = 0.8 a_t \sigma_u D + 0.5 N D [ 1 - N / (B D F_c) ] \quad (3.3)$$

where  $M_y$  and  $M_u$  are the flexural yield strength and the ultimate flexural strength, respectively;  $\sigma_y$  and  $\sigma_u$  are the yield strength and the tensile strength of rebar, respectively;  $a_t$  is the cross-sectional area of tensile rebars;  $B$ ,  $D$ , and  $d$  are the width, the depth, and the effective depth of a section, respectively;  $F_c$  is the compressive strength of concrete; and  $N$  is the axial load.

Equation 3.1 and Eqn. 3.2 are applied in calculating lateral resistance of RC fence walls and RC seawalls, and Eqn. 3.3 is applied in calculating lateral resistance of RC columns.  $M_{OT}$  is applied for the overturned structures such as gravity-type seawalls, gate piers, stone monuments, etc. and  $P_s$  is applied for the slid stone monument. The buoyant force is neglected in calculating  $M_{OT}$  and  $P_s$  herein, because it is negligibly small when a tsunami applies impulsive force to a structure.

## 4. COMPARISON BETWEEN TSUNAMI LOAD AND OBSERVED DAMAGE

### 4.1. Drag Force Evaluation

The guidelines (JCO 2005) introduce the design tsunami load (described later), which is supposed to be applied for impulsive force on onshore structures. However the 2011 Great East Japan Earthquake evidenced through numerous recorded videos that structures were gradually inundated and may have been affected more significantly by drag force rather than impulsive force. Therefore, in this paper, the tsunami load is evaluated based on drag force and compared to the design tsunami load introduced by the guidelines (JCO 2005).

The drag forces  $F_D$  is generally expressed by Eqn. 4.1.

$$F_D = \frac{1}{2} \rho C_D u^2 A_D \quad (4.1)$$

where  $F_D$  (kN) is the drag force;  $\rho$  ( $\text{t/m}^3$ ) is the mass per unit volume of water (1.0 assumed herein);  $C_D$  is the drag coefficient;  $u$  ( $\text{m/s}$ ) is the flow velocity; and  $A_D$  ( $\text{m}^2$ ) is the loaded area of a structure in the plane normal to the direction of flow. Assuming the drag coefficient  $C_D$  2.0 for the quadrilateral structures surveyed (JSCE 1971), Eqn. 4.1 leads to Eqn. 4.2.

$$F_D = \rho u^2 A_D \quad (4.2)$$

Assuming that the tsunami pressure is uniformly distributed as shown in Fig. 2, the pressure  $\omega_R$  under which the overall tsunami load is equal to the structure's strength considering their failure mechanism is obtained. Then the tsunami load  $V$  equal to the structure's strength is expressed by Eqn. 4.3. Note that the tsunami pressure above the structures is neglected as shown in case 2 of Fig. 2.

$$V = \omega_R A_D \quad (4.3)$$

Setting  $F_D$  equal to  $V$ , the flow velocity  $u_R$  equivalent to the structure's strength is expressed by Eqn. 4.4.

$$u_R = \sqrt{\omega_R / \rho} \quad (4.4)$$

Then the Froude number  $Fr_R$  equivalent to the structure's strength is expressed by the equivalent flow velocity  $u_R$  and the measured tsunami inundation depth  $\eta_m$  (Eqn. 4.5).

$$Fr_R = \frac{u_R}{\sqrt{g\eta_m}} = \frac{\sqrt{\omega_R / \rho}}{\sqrt{g\eta_m}} \quad (4.5)$$

From the discussion above, the equivalent flow velocity  $u_R$  and the Froude number  $Fr_R$  are obtained from Eqn. 4.4 and Eqn. 4.5 using the equivalent tsunami pressure  $\omega_R$ . To estimate the actual tsunami

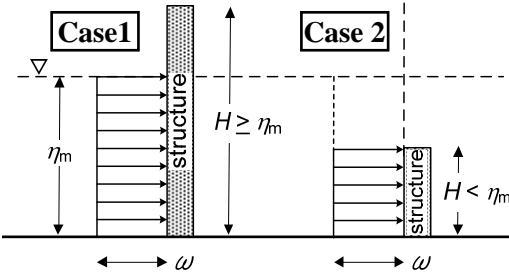


**Figure 2.** Measured inundation depth  $\eta_m$ , structure's height  $H$ , and tsunami pressure distribution  $\omega$

pressure, flow velocity, and Froude number, the equivalent values to discriminate between collapsed and survived structures are estimated as discussed earlier.

#### 4.2. Tsunami Load Evaluation Based on Relationship between Structure's Damage and Drag Force

Of all surveyed structures, 43 simple structures and 8 RC buildings are employed to estimate the tsunami pressure, flow velocity, and Froude number. Assuming that the tsunami load differs depending on the site environment, the structures are divided into two groups, i.e., those in areas with or without structures on the sea side that are deemed effective to reduce the tsunami power such as breakwater. Then they are plotted from north to south in Fig. 3, starting from left, showing their structural type and the observed failure mode: “Y”, “U”, “S”, and “O” correspond to rebar yielding, rebar fracture resulting in ultimate strength, sliding, and overturning, respectively. Dashed lines in Fig. 3 show the boundary between ria coast area (Sanriku area) and flatland area such as Sendai plain.

In this paper, the areas with structures to reduce the tsunami power include Kamaishi city, Ofunato city, and Onagawa town where breakwaters are provided at its bay mouth; Rikuzentakata city, Ishinomaki city, Sendai city, etc. where breakwaters and seawalls which are considered high enough to reduce the tsunami power are provided; Kesen-numa city where the bay holds Hachigasaki area off the coast which served as a natural breakwater.

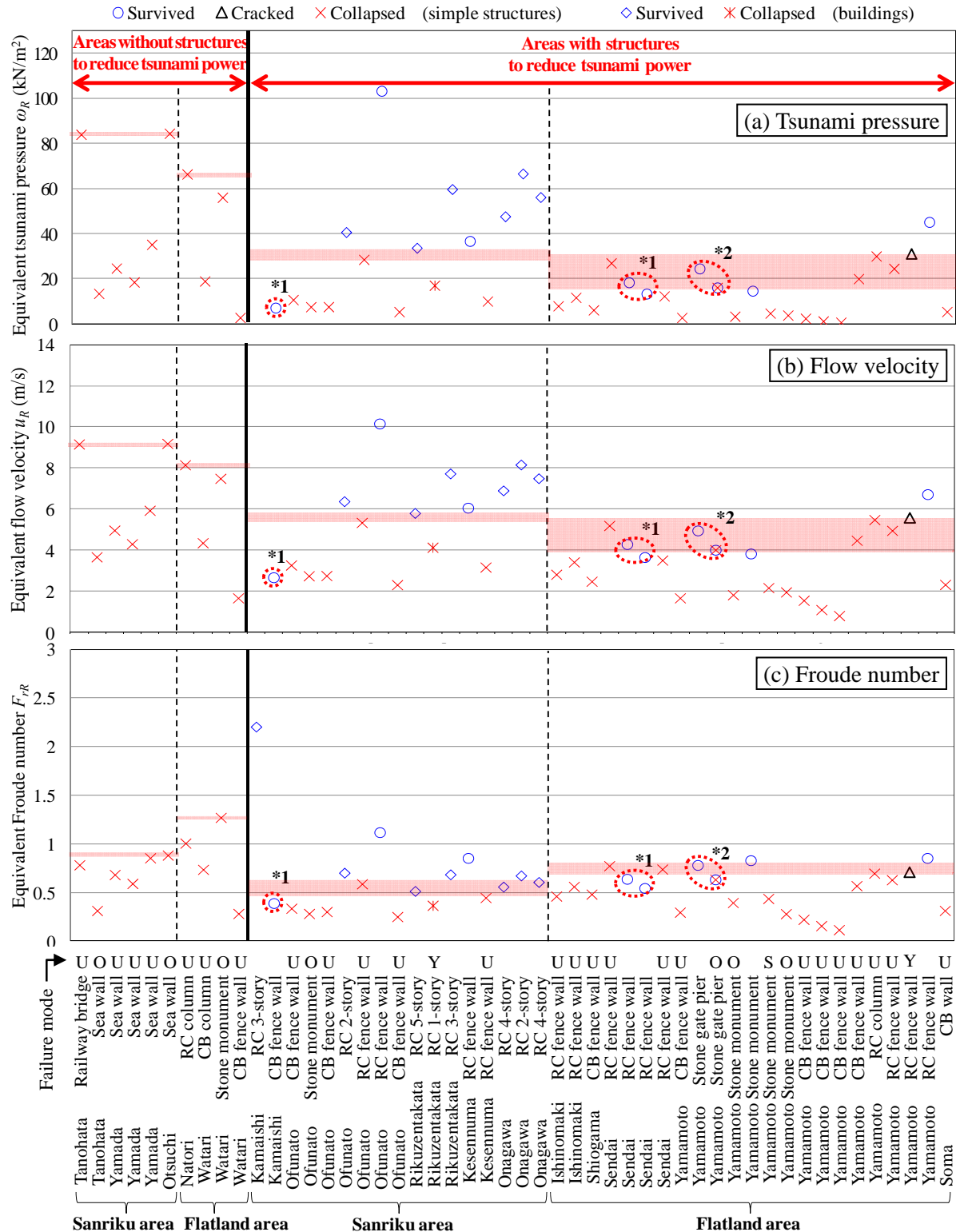
The vertical axis in Fig. 3 shows the equivalent tsunami pressure  $\omega_R$ , flow velocity  $u_R$ , and Froude number  $F_{rR}$  obtained from Eqns. 4.3, 4.4, and 4.5. Each plot in Fig. 3 explains that the collapsed structures (designated as  $\times$  and  $*$ ) were exposed to the force higher than the drag force due to the tsunami pressure  $\omega_R$ , flow velocity  $u_R$ , and Froude number  $F_{rR}$  (derived from the structure's strength) plotted in the vertical axis, while the survived structures (designated as  $\circ$  and  $\diamond$ ) were exposed to the force lower than that, and the cracked structures (designated as  $\Delta$ ) were just exposed to the drag force due to  $\omega_R$ ,  $u_R$ , and  $F_{rR}$ . Note that the data denoted by \*1 are structures oriented parallel to the direction of the tsunami flow and survived despite the equivalent tsunami pressure  $\omega_R$ , flow velocity  $u_R$ , and Froude number  $F_{rR}$  were *smaller* (i.e., structurally weaker) than that of the other survived structures due to their actual loaded areas smaller than assumed in the calculation. Also note that the structures denoted by \*2 are stone gate piers embedded in the ground but its contribution to the overturning resistance is neglected for simple calculation and therefore their actual  $\omega_R$ ,  $u_R$ , and  $F_{rR}$  shuold be larger than the value shown in Fig. 3. Considering those mentioned above, the boundary values to discriminate between collapsed ( $\times$  and  $*$ ) and survived ( $\circ$  and  $\diamond$ ) structures are found and hatched to estimate the tsunami pressure, flow velocity, and Froude number as shown in Fig. 3. Note that the hatched horizontal lines in the area without structures to reduce the tsunami power corresponds to the lower bound because no data on survived structure in the area are available in this study.

The tsunami pressure acted on the structures, as shown in Fig. 3(a), is more than  $85\text{kN/m}^2$  where they have no structures to reduce the tsunami power, while it lies in the range of 15 to  $30\text{kN/m}^2$  where they have structures to reduce the tsunami power, excluding the data denoted by \*1.

The flow velocity, as shown in Fig. 3(b), is more than 9m/s where they have no structures to reduce the tsunami power, while it lies in the range of 4 to 6m/s where they have structures to reduce the tsunami power. To validate the estimated flow velocity in Fig. 3(b), it is compared to the velocity of the floating objects recorded in the tsunami videos in the following 7 points: Kamaishi city (2 points), Ofunato city (2 points), Onagawa town (2 points) in Sanriku area and Natori city (1 point) in flatland area. All of them have structures to reduce tsunami power such as breakwaters or seawalls. Note that one record in Onagawa town corresponds to the second or later attack, while the other 6 records are confirmed the first attack since the first arrival of tsunami is recorded. The measured velocities are plotted in Fig. 4 only when the floating objects appear on the videos. As can be found in Fig. 4, the flow velocity lies in the range of 3 to 6m/s regardless the inundation depth and consistent with the estimated result (4 to 6m/s) based on drag force.

The Froude number  $F_r$ , as shown in Fig. 3(c), is more than 1.27 where they have no structures to

reduce tsunami power. On the other hand, it lies in the range of 0.5 to 0.65 in Sanriku area and it is around 0.8 in flatland area where they have structures to reduce the tsunami power. The Froude numbers in Sanriku area is rather smaller than that in flatland area with structures to reduce tsunami



\*1 Structures oriented parallel to the direction of the tsunami flow and survived despite their  $\omega_R$ ,  $u_R$ , and  $F_{Rr}$  were smaller (i.e., structurally weaker) than that of the other survived structures.

\*2 Stone gate piers embedded in the ground but its contribution to the overturning resistance is neglected for simple calculation and therefore their actual  $\omega_R$ ,  $u_R$ , and  $F_{rR}$  should be larger than the value shown in the vertical axis.

**Figure 3.** Relationship between equivalent tsunami pressure, flow velocity, Froude number and structure's damage

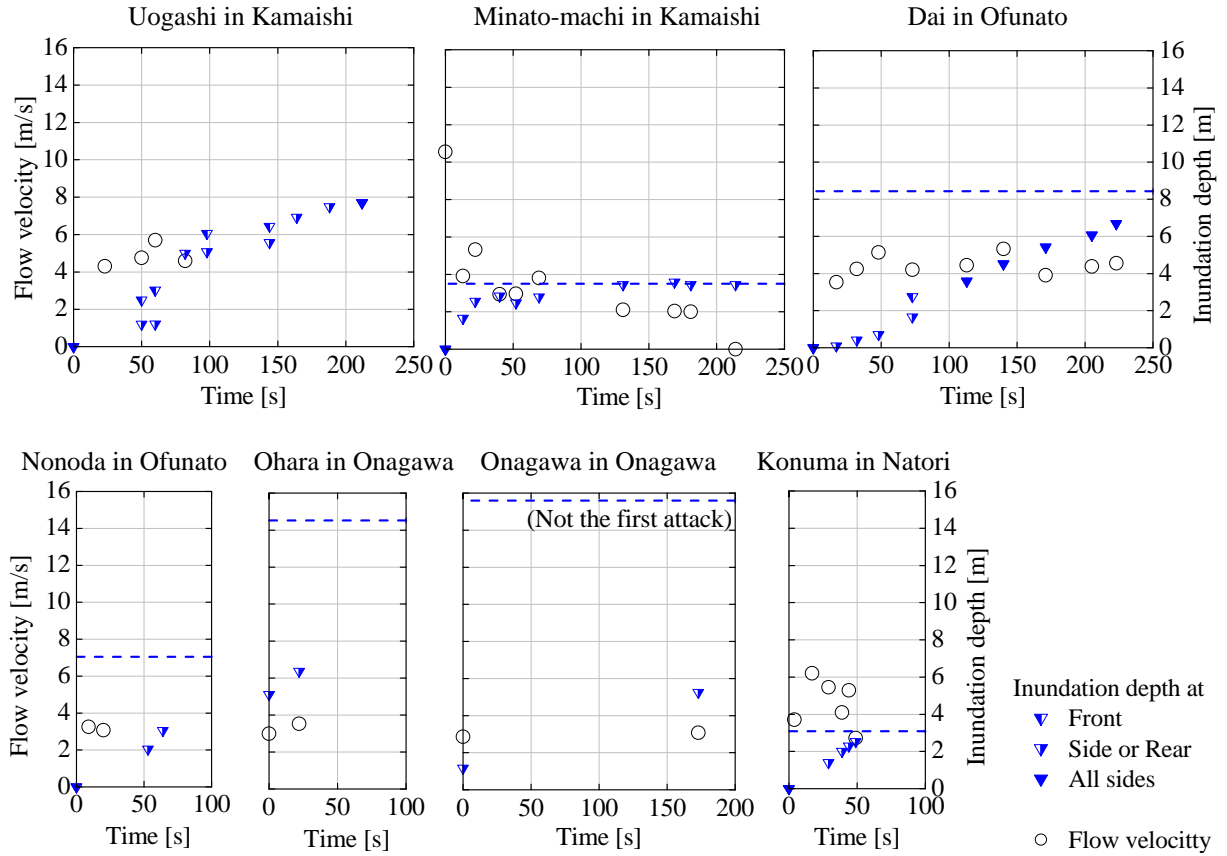


**Figure 4.** Measured flow velocity and inundation depth derived from the tsunami recorded videos

power although the flow velocity in Sanriku area is the same or even higher than that in flatland area. Therefore, the flow velocity in Sanriku area is found not so high despite the high inundation depth.

#### 4.3. Comparison with Design Tsunami Load

Since the estimated flow velocity is found consistent with that derived from the tsunami recorded videos, the tsunami load evaluated based on drag force is compared to the design tsunami load introduced by the guidelines (JCO 2005).

In the guidelines (JCO 2005), the design tsunami load is defined by Eqn. 4.6. In this discussion, Eqn. 4.7 that is analogous to Eqn. 4.6 is first defined (Nakano 2008), and the water depth coefficient  $a$  is evaluated based on the Froude number estimated in the previous section:

$$q_z = \rho g (3h - z) \quad (0 \leq z \leq 3h) \quad (4.6)$$

$$p_z = \rho g (a\eta_m - z) \quad (0 \leq z \leq a\eta_m) \quad (4.7)$$

where  $q_z$  ( $\text{kN/m}^2$ ) is the design tsunami pressure acting on a structure at a distance  $z$  (m) above the ground level defined in the guidelines (JCO 2005);  $\rho$  ( $\text{t/m}^3$ ) is the mass per unit volume of water (1.0 assumed herein);  $g$  ( $\text{m/s}^2$ ) is the gravity acceleration;  $h$  (m) is the design tsunami inundation depth;  $p_z$  ( $\text{kN/m}^2$ ) is the tsunami pressure acting on a structure at a distance  $z$  (m) above the ground level defined in this study to investigate a rational value of  $a$ ;  $\eta_m$  (m) is the measured tsunami inundation depth; and  $a$  is the water depth coefficient.

Figure 5 illustrates the background concept employed in Eqn. 4.6. The design tsunami pressure distribution acting along the structure's height is assumed a triangular shape with the height reaching 3 times of the design tsunami inundation depth  $h$  (i.e., the pressure at the bottom is assumed 3 times of the hydrostatic pressure) based on the experimental results (Asakura et al. 2000).

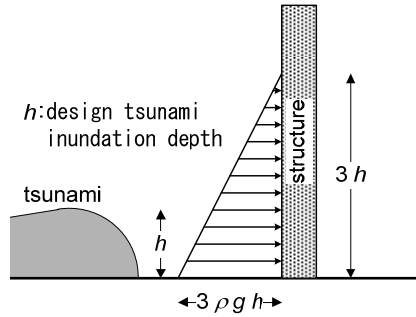


**Figure 5.** Design tsunami pressure distribution (JCO 2005)

Given that the equivalent water depth  $a\eta_m$  is lower than a structure with no openings, the wave force  $F_x$  under a triangular hydrostatic pressure profile by Eqn. 4.7 and the drag force  $F_D$  can be expressed as Eqn. 4.8 and Eqn. 4.9, respectively, for a unit width (1m) of a structure.

$$F_x = \frac{1}{2}(a\eta_m \times 1)a\rho g\eta_m = \frac{a^2}{2}\eta_m^2 \rho g \quad (4.8)$$

$$\begin{aligned} F_D &= \rho u^2 A_D \\ &= \rho u^2(\eta_m \times 1) = F_r^2 \eta_m^2 \rho g \end{aligned} \quad (4.9)$$

Setting  $F_x$  equal to  $F_D$ , Eqn. 4.10 is obtained. Then the relationship between the coefficient  $a$  and Froude number  $F_r$  is expressed by Eqn. 4.11.

$$\frac{a^2}{2} = F_r^2 \quad (4.10)$$

$$a = \sqrt{2} \times F_r \quad (4.11)$$

From Eqn. 4.11, the coefficient  $a$  is computed based on the Froude number.

Figure 6 shows the relationship between the coefficient  $a$  obtained from Eqn. 4.11 and the measured tsunami inundation depth  $\eta_m$  for each area with different site environment. Fig. 6(a) and Fig. 6(b) show that the coefficient  $a$  to discriminate between collapsed and survived structures is above 1.3 and 1.8 in Sanriku area and flatland area, respectively, without structures to reduce the tsunami power. Note that the upper bound of the coefficient  $a$  cannot be determined from Fig. 6(a) and Fig. 6(b) because survived structures are not plotted in these Figures. Fig. 6(c) shows that the coefficient  $a$  to discriminate between collapsed and survived structures is around 0.9 in Sanriku area with structures to reduce the tsunami power when the measured tsunami inundation depth  $\eta_m$  is smaller than 10m. Fig. 6(c) also shows that the buildings whose coefficient  $a$  is much smaller than 1 survived when  $\eta_m$  is larger than 13m. It implies that the tsunami load was smaller than the hydrostatic force of inundation depth  $\eta_m$ , because the water had flown all around the buildings when the inundation depth reached  $\eta_m$  and loaded on all sides of the building. Fig. 6(d) shows that the coefficient  $a$  to discriminate between collapsed and survived structures is around 1.1 in flatland area with structures to reduce the tsunami power.

It should be noted that the results based on the damage observations after the 2004 Indian Ocean Tsunami (Nakano 2008) concluded that the boundary coefficient  $a$  lies in the range of 2 to 2.5, which is much larger than the result obtained in this study. This is probably because structures investigated after the Indian Ocean Tsunami were located just close to the coastlines with no built environment to reduce tsunami power and high tsunami waves directly attacked the structures.

Table 1 summarizes the results found in the above discussions.

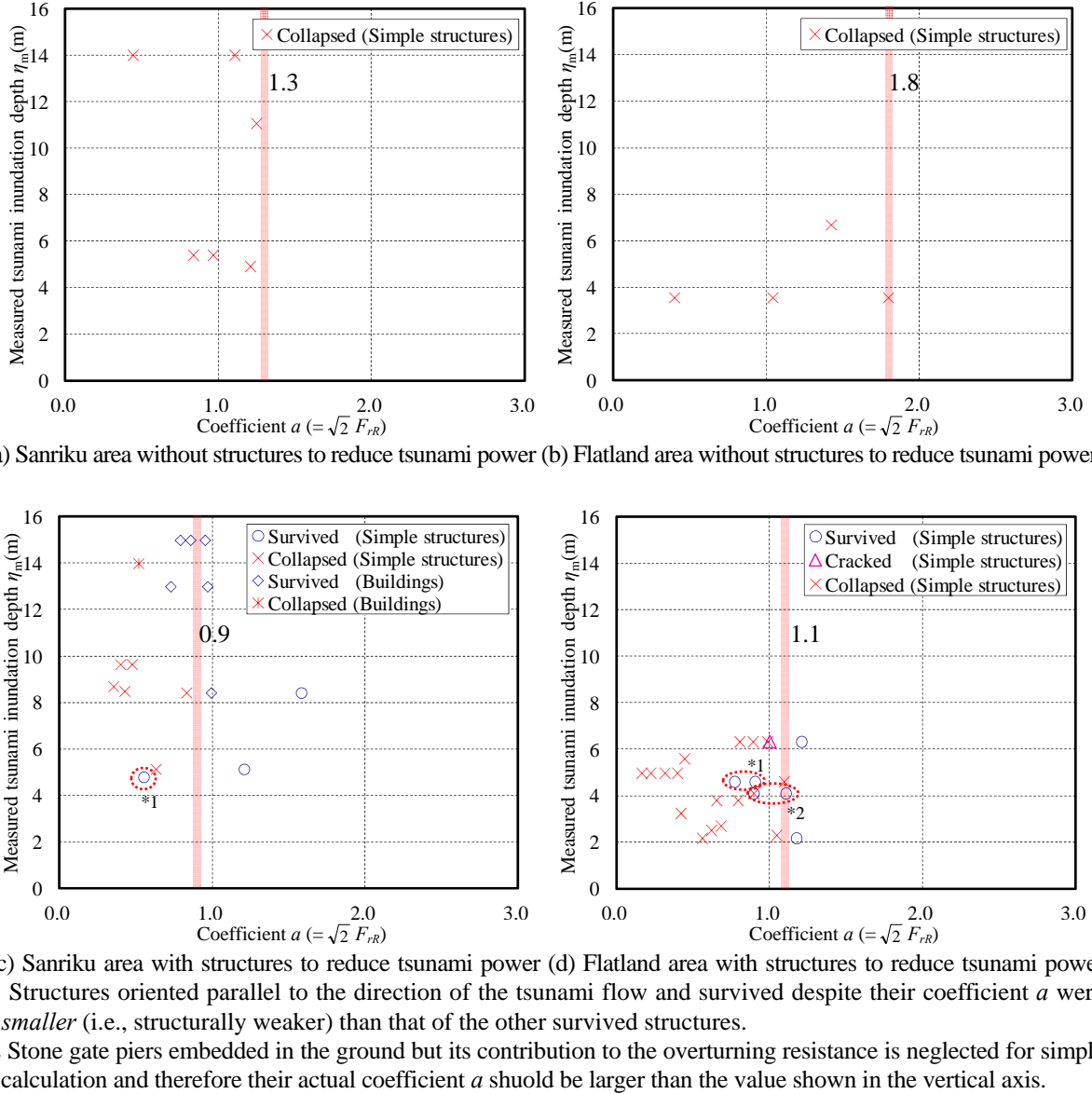


**Figure 6.** Computed coefficient  $a$  vs. measured tsunami inundation depth  $\eta_m$

**Table 1.** Coefficient  $a$  to discriminate collapsed and survived structures

	Areas with structures to reduce tsunami power		Areas without structures to reduce tsunami power	
	Sanriku area	Flatland area	Sanriku area	Flatland area
Coefficient $a$ ( $= \sqrt{2} F_r$ )	0.9	0.9	1.1	$\geq 1.3$
				$\geq 1.8$

## 6. CONCLUSIONS

To verify the design load specified in the Japanese guidelines for tsunami shelters, the tsunami load is evaluated based on the damage observations after the 2011 Great East Japan Earthquake. The major findings can be summarized as follows:

1. The tsunami pressure, the flow velocity, and the Froude number are more than  $85\text{kN/m}^2$ ,  $9\text{m/s}$ , and  $1.27$  respectively, in the areas without structures to reduce the tsunami power. In the areas with structures to reduce the tsunami power, they lie in the range of  $15$  to  $30\text{kN/m}^2$ ,  $4$  to  $6\text{m/s}$ , and  $0.5$  to  $0.65$  in Sanriku area and  $0.8$  in flatland area, respectively.

2. The water depth coefficient  $a$  computed in terms of the Froude number is larger than 1.3 and 1.8 in Sanriku area and flatland area, respectively, without structures to reduce the tsunami power, while it is around 0.9 in Sanriku area (or smaller especially when  $\eta_m$  is larger than 10m) and 1.1 in flatland area, respectively, with structures to reduce the tsunami power.
3. The coefficient  $a$  obtained in this study is much smaller than those obtained from the damage observations after the 2004 Indian Ocean Tsunami. This is probably because structures investigated after the Indian Ocean Tsunami were located just close to the coastlines with no built environment to reduce tsunami power and high tsunami waves therefore directly attacked the structures.
4. It should be noted therefore that the design lateral load for tsunami shelters should be determined further considering evidences obtained in other events and experimental researches as well as those found in this study.

#### **ACKNOWLEDGMENT**

This paper includes discussions made under “Investigation on Building Code Development in Tsunami Hazard Areas,” granted by the Ministry of Land, Infrastructure, Transport and Tourism (Principal Investigator: Yoshiaki NAKANO, Professor at IIS, The University of Tokyo). The field surveys and investigations were partially supported by the General Insurance Association of Japan granted for the research to review earthquake damage insurance guidelines for RC buildings. The surveys were made under extensive cooperation with Prof. Nishida T. et al. of Akita Prefectural University, Research Associates Takahashi N. and Choi H. et al. of IIS, The University of Tokyo. The authors gratefully acknowledge their valuable supports to complete the research project.

#### **REFERENCES**

- Asakura, R., Iwase, K., Ikeya, T., Takao, M., Kaneto, T., Fujii, N. and Omori, M. (2000). An Experimental Study on Wave Force Acting on On-Shore Structures due to Overflowing Tsunamis. *Proceedings of Coastal Engineering*, Japan Society of Civil Engineers, **47**, 911-915. (in Japanese)
- JBDP/The Japan Building Disaster Prevention Association (1977, 1990, and 2001(in Japanese) and 2005 (in English)). *Standard for Seismic Evaluation of Existing Reinforced Concrete Buildings*.
- JCO/Task Committee under the Japanese Cabinet Office (2005). *Design Guidelines for Tsunami Shelters*. (in Japanese), <http://www.bousai.go.jp/oshirase/h17/050610/guideline.pdf>
- JSCE/Japan Society of Civil Engineers (1971). *Hydraulic Formula*. (in Japanese)
- Nakano, Y. (2008). Design load evaluation for tsunami shelters based on damage observations after Indian Ocean Tsunami disaster due to the 2004 Sumatra Earthquake. *The 14th World Conference on Earthquake Engineering*, Paper ID 15-0008
- Okada, T., Sugano, T., Ishikawa, T., Ogi, T., Takai, S. and Hamabe, T. (2004a). Structural Design Method of Building to Seismic Sea Wave, No. 1 Preparatory Examination. *Building Letter*, The Building Center of Japan (in Japanese)
- Okada, T., Sugano, T., Ishikawa, T., Ogi, T., Takai, S. and Hamabe, T. (2004b). Structural Design Method of Building to Seismic Sea Wave, No. 2 Design Method (a Draft). *Building Letter*, The Building Center of Japan (in Japanese)